

# Tiny-PULP-Dronets: Squeezing Neural Networks for Faster and Lighter Inference on Multi-Tasking Autonomous Nano-Drones

Lorenzo Lamberti\*, Vlad Niculescu†, Michał Barcis‡, Lorenzo Bellone‡, Enrico Natalizio‡, Luca Benini\*†, Daniele Palossi†§

\* Department of Electrical, Electronic and Information Engineering - University of Bologna, Italy

† Integrated Systems Laboratory - ETH Zürich, Switzerland

‡ Autonomous Robotics Research Center - Technology Innovation Institute, UAE

§ Dalle Molle Institute for Artificial Intelligence - USI and SUPSI, Switzerland

lorenzo.lamberti@unibo.it, vladn@iis.ee.ethz.ch, michal.barcis@tii.ae, lorenzo.bellone@tii.ae, enrico.natalizio@tii.ae, luca.benini@unibo.it, daniele.palossi@idsia.ch

**Abstract**—Pocket-sized autonomous nano-drones can revolutionize many robotic use cases, such as visual inspection in narrow, constrained spaces and ensure safer human-robot interaction due to their tiny form factor and weight – i.e., tens of grams. This compelling vision is challenged by the high level of intelligence needed aboard, which clashes against the limited computational and storage resources available on PULP (parallel-ultra-low-power) MCU class navigation and mission controllers that can be hosted aboard. This work moves from PULP-Dronet, a State-of-the-Art convolutional neural network for autonomous navigation on nano-drones. We introduce Tiny-PULP-Dronet: a novel methodology to squeeze by more than one order of magnitude model size ( $50\times$  fewer parameters), and number of operations ( $27\times$  less multiply-and-accumulate) required to run inference with similar flight performance as PULP-Dronet. This massive reduction paves the way towards affordable multi-tasking on nano-drones, a fundamental requirement for achieving high-level intelligence.

## I. INTRODUCTION

With their sub-10 cm diameter and tens of grams in weight, nano-UAVs are agile and highly versatile robotic platforms, employed in many use cases where small size is crucial. From aerial inspection in narrow and dangerous places [1] to close-proximity human-robot interaction tasks [2], nano-UAVs are the ideal candidate platforms. Similar to other autonomous robots, also nano-UAVs navigate thanks to the interaction of three key sub-systems [3]. The *state estimator* determines the current state of the system. Then, what we call the onboard *intelligence* is responsible for solving the decision-making problem of choosing the next target state. Finally, the *control* part brings the system from the current state to the target one. Our work focuses on the intelligence, where the limited payload and power density of nano-drones clash with the onboard execution of complex real-time algorithms and even more with multi-tasking vision-based solutions.

Therefore, our goal is to minimize the onboard intelligence workload. This scenario allows to optimally balance between *i)* enhancing the UAV’s reactivity with an increased throughput in the decision-making process [4], and *ii)* freeing up resources

for the execution of multi-perception intelligence tasks aboard our nano-drone. These features enable nano-UAVs to tackle more complex flight missions. For example, autonomous aerial cinematography and high-speed drone racing require a combination of multiple tasks running concurrently aboard [5], [6], including visual-inertial odometry, object detection, trajectory planning, environment mapping, and collision avoidance. Ultimately, we could significantly push small-size robotic platforms towards the biological levels of intelligence [7].

To date, nano-drones can accomplish individual intelligence autonomous navigation tasks by leveraging deep learning-based (DL) algorithms – spanning a broad spectrum of complexity and sensorial input [2], [8]–[10]. In [8], Kooi and Babuška use a deep reinforcement learning approach with proximal policy optimization for the autonomous landing of a nano-drone on an inclined surface. The designed convolutional neural network (CNN) requires about 4.5k multiply-accumulate (MAC) operations per forward step, being sufficiently small to allow a single action evaluation in about 2.5 ms on a single-core Cortex-M4 processor, but still providing limited perception capabilities, restricted to landing purposes only. Employing the same Cortex-M4, Neural-Swarm2 [9] exploits a DL-based controller to compensate close-proximity interaction forces that arise in formation flights of nano-drones. With only about 37kMACs, each nano-drone processes only the relative position and velocity of surrounding UAVs, enabling safe close-proximity flight.

Focusing on higher complexity DL-based workloads, the computational limitations imposed by single-core MCUs can be addressed by leveraging cutting-edge flight controllers targeting artificial intelligence. An example of these new-generation devices is given by the 9-core GWT GAP8<sup>1</sup>, a parallel-ultra-low-power (PULP) processor. This processor was previously exploited on UAVs in the PULP-Dronet project [10], leading to a fully-programmable end-to-end visual-based autonomous navigation engine for nano-drones.

<sup>1</sup>[https:// greenwaves-technologies.com/gap8\\_mcu\\_ai](https://greenwaves-technologies.com/gap8_mcu_ai)

PULP-Dronet is a single CNN capable of navigating a 27-grams nano-drone in both indoor and outdoor environments by predicting a collision probability, for obstacle avoidance, and a steering angle, to keep the drone within a lane. Similarly, in the PULP-Frontnet project [2] the PULP paradigm is leveraged to successfully run a lightweight CNN (down to 4.8 MMAC and 78 kB) that performs a real-time relative pose estimation of a free-moving human, on a nano-UAV. This prediction is then fed to the nano-drone’s controller, enabling precise “human following” capability. Both PULP-Dronet and PULP-Frontnet demonstrate the feasibility of embedding high-level intelligence aboard nano-UAVs. However, all these State-of-the-Art (SoA) solutions focus on vision-based single task intelligence, as the computational/memory burden for multi-tasking perception is still challenging ultra-low-power MCUs.

This paper presents a general methodology for analyzing the size and complexity of deep learning models suffering from *overfitting* and *sparsity*, which we apply, as an example, to the SoA PULP-Dronet CNN. Then, we study the various trade-offs between the number of channels, pruning of inactive neurons, and accuracy, demonstrating the effectiveness of our method by introducing novel squeezed versions of the PULP-Dronet called Tiny-PULP-Dronets. Our CNNs are up to  $50\times$  smaller and  $8.5\times$  faster than the baseline running on the same PULP GAP8 SoC, with no compromise on the final regression/classification performance. Ultimately, the Tiny-PULP-Dronets, with a minimum model size of only 6.4 kB and a maximum throughput of more than 160 frame/s, enable higher reactivity on the autonomous navigation task, and leave sufficient memory and compute headroom for onboard multi-tasking intelligence even at the nano-sized scale.

## II. METHODOLOGY

PULP-Dronet [10] is a ResNet-based [11] CNN made of three residual blocks (ResBlocks), where each one consists of a main branch, performing two  $3 \times 3$  convolutions, and a parallel by-pass (Byp), performing one  $1 \times 1$  convolution. This CNN produces a steering angle (regression) and a collision probability (classification) output. Therefore, the model is trained using two different metrics: the mean squared error (MSE) and the binary cross-entropy (BCE). The two metrics are then combined in a single loss function,  $Loss = MSE + \beta BCE$ , where  $\beta$  is set to 0 for the first 10 epochs, gradually increasing in a logarithmic way to prioritize the regression problem. Finally, the training process exploits a dynamic *negative hard-mining* procedure, gradually narrowing down the loss computation to the k-top samples accounting for the highest error.

PULP-Dronet is deployed in fixed-point arithmetic on a multi-core GAP8 SoC, yielding 41 MMAC operations per frame and 320 kB of weights. The peak memory footprint – also including input and intermediate buffers – is as much as 400 kB, which is close to the total on-chip L2 memory (i.e., 512 kB) and represents a strong limiting factor for our multi-tasking objective.

**Overfitting.** A strong indicator of a deep learning model’s overfitting is a decreasing/constant training loss paired with

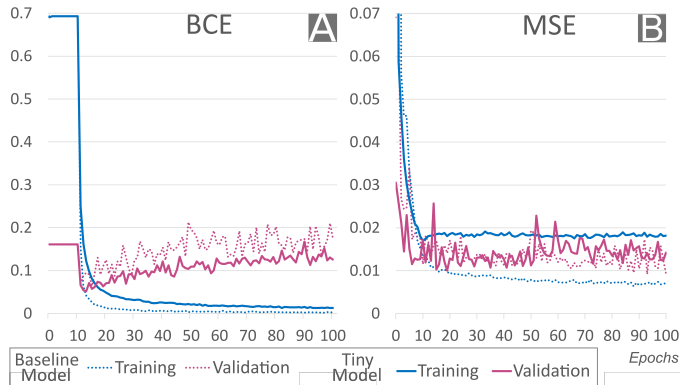


Figure 1. Training/validation loss’ components – BCE (A) and MSE (B) – of PULP-Dronet, comparing the the baseline model against the tiny one.

a validation loss that grows over the epochs. In Figure 1, we show both BCE (A) and MSE (B) curves over 100 epochs for both training (64 k images) and validation (7 k images) procedure. In Figure 1-A, the *baseline* PULP-Dronet (dotted lines) suffers from overfitting on the BCE, showing a constantly growing validation error, while the MSE (Figure 1-B) shows a noisy but almost constant validation error trend. This behavior gives us the intuition that the network topology could be over-parameterized for the given perception problem.

Therefore, we introduce a model exploration to minimize its size while aiming at the same minimum in the validation losses – or even lower. Our approach aims at thinning the network’s tensors by applying a  $\gamma$  scaling factor to the number of channels across all layers. We span the  $\gamma$  parameter in the range  $[0.125, 0.250, 0.5, 1.0]$ , where  $\gamma = 1.0$  corresponds to the baseline PULP-Dronet, and we call the smaller variants Tiny-PULP-Dronet CNNs. The smallest Tiny-PULP-Dronet ( $\gamma = 0.125$ ) losses are reported in Figure 1 (solid lines), where both the baseline and the tiny model assess to the same minimum validation MSE of 0.01. On the other hand, the tiny model achieves a minimum validation BCE of 0.052, slightly lower than the corresponding value of the baseline (0.064), confirming overfitting of the baseline PULP-Dronet.

**Sparsity.** Deep learning models’ sparsity analysis is a key tool for identifying and selectively pruning parts of the models that are not contributing to the learning process [12]. We define as the *structural activation’s sparsity* the percentage of neurons in a convolutional layer that never activate over the entire validation dataset – always equal to 0. This analysis for the PULP-Dronet baseline is reported in Table I, which highlights significant sparsity across the whole network, peaking in the ResBlock3 (92% for the last by-pass). These results suggest: *i*) the network might suffer of over-parametrization, across all layers; and *ii*) by-pass branches, usually exploited in very deep CNNs to avoid *vanishing gradient* effects [11], are underutilized in this shallow CNN.

Therefore, we analyze the gradients for each network layer after the by-pass removal: the convolution associated with Act1 shows the strongest gradient’s attenuation. On this layer, we record on the last 10 epochs (worst case) an average

TABLE I  
STRUCTURAL SPARSITY ANALYSIS OF PULP-DRONET, COMPARING THE  
BASELINE VS. THE TINY MODEL.

Topology	Conv		ResBlock1			ResBlock2			ResBlock3		
	Act0	Act1	Act2	Byp1	Act3	Act4	Byp2	Act5	Act6	Byp3	
Baseline	28%	13%	6%	6%	25%	10%	11%	49%	60%	92%	
Tiny	0.15%	0%	0%	—	0%	0.07%	—	0%	0%	—	

gradient magnitude of 0.055 with a standard deviation of 0.16, supporting the initial intuition of no vanishing gradients on the PULP-Dronet shallow CNN. Furthermore, in Table I, we also provide the same sparsity analysis for the smallest Tiny-PULP-Dronet ( $\gamma = 0.125$ ), with by-pass branches removed. Compared to the baseline model, the tiny one scores a sparsity of almost 0% across all layers, suggesting a more efficient usage of the neurons left after the two squeezing techniques.

### III. RESULTS

#### A. Models evaluation

In this section, we present our study on the effect of the proposed methodology when applied to the PULP-Dronet CNN in terms of memory footprint, computational effort, and regression/classification performance. Figure 2 presents the comparison between the baseline CNN against its Tiny variants. The reduction of the number of channels through  $\gamma$  saves 237–314 kB and 29–39 MMAC. Additionally, also the by-pass removal reduces the memory usage of 1–12 kB and the operations by 0.1–1 MMAC, depending on the specific model. Combining by-pass removal and the scaling of network’s channels, the smallest Tiny-PULP-Dronet reduces 50 $\times$  memory footprint and 27 $\times$  on MAC operations vs. the baseline, reaching a minimum of 6.4 kB and 1.5 MMAC, respectively.

Focusing on the regression performance for the testing set, the root mean squared error (RMSE) shows a similar trend for both *with* and *without* (w/o) by-pass groups (Figure 2). The score slowly improves while reducing the model size from  $\gamma = 1$  to  $\gamma = 0.25$ , which is a common behavior of those models that suffer from overfitting and take advantage of an increased generalization capability, reducing their trainable parameters [12]. Instead, for both groups, the smallest models ( $\gamma = 0.125$ ) show a lower improvement on the RMSE, suggesting their potential underfitting. Figure 2 also reports the Accuracy evaluation for the classification problem. While this metric, on the *with by-pass* group, seems to keep an almost constant performance all over the sizes ( $\sim 0.91$ ), it slowly reduces with the size for the *without by-pass* group. Overall, the by-pass removal does not significantly penalize either the RMSE or the Accuracy of the models, allowing to reach a remarkable 0.88 Accuracy for the smallest configuration. More importantly, this pruning is highly desirable for *i*) reducing the memory footprint ( $\sim 3\%$ ) and operations ( $\sim 1.5\%$ ), and *ii*) simplifying the deployment process on MCUs.

To support the second point, we further analyze the peak memory allocation needed for one single-image inference of the CNNs accounting for input/output intermediate buffers

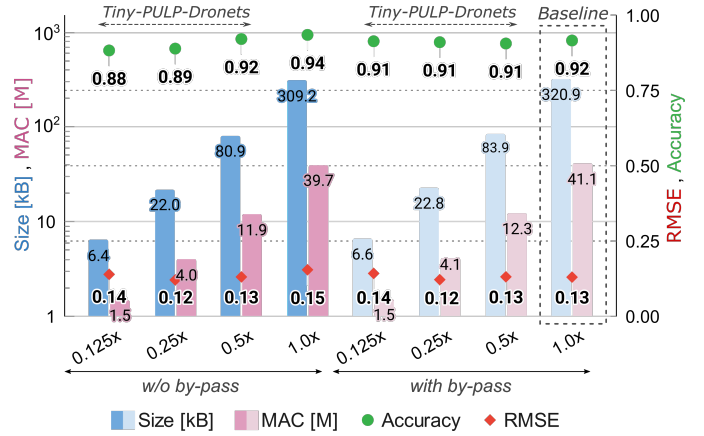


Figure 2. Comparing PULP-Dronet vs. its Tiny variants, in terms of size, MAC, Accuracy, and RMSE. We span  $\gamma$  in the  $[0.125, 0.250, 0.5, 1.0]$  range.

and network weights. Looking at the peak memory allocation utilizing a simple *incremental allocator*, which sums up the memory required by each layer, the baseline PULP-Dronet requires 870 kB compared to only 105 kB for the smallest Tiny-PULP-Dronet ( $\gamma = 0.125$ ). On the other hand, by employing a *dynamic allocator* which maximizes data reuse, the baseline PULP-Dronet peaks at 400 kB, while the smallest CNN peaks at 80.1 kB. In this latest case, the removal of by-pass branches simplifies and reduces the memory burden eliminating the need for the simultaneous storage of two intermediate activations along parallel branches, which peaks at 10 kB in the smallest Tiny-PULP-Dronet. Considering the dynamic allocator, we ultimately reduce by 5 $\times$  the peak memory usage required by the onboard intelligence, a key element to enable multi-tasking aboard constrained devices like the GAP8 SoC.

#### B. Power analysis

We evaluate GAP8’s execution time and energy consumption when running a single-frame inference with the smallest Tiny-PULP-Dronet model ( $\gamma = 0.125$ ). We use the RocketLogger data logger [13] (64 ksp/s) to separately plot the power waveforms of the GAP8’s main core, the Fabric Controller (FC), and its 8-core parallel cluster (CL). We test two SoC configurations: the so called energy-efficient configuration [10], whose operating point is FC@50 MHz, CL@100 MHz, and VDD@1 V, and the maximum performance settings according to the GAP8’s datasheet, which is FC@250 MHz, CL@175 MHz, VDD@1.2 V.

GAP8 takes 1.1 Mcycles to process the Tiny-PULP-Dronet, as shown with the power traces in Figure 3, where we highlight the individual execution of each network’s layer, for both SoC configurations. The energy-efficient configuration (Figure 3-A) shows an average power consumption of 34 mW, 11.3 ms inference time, for a total energy consumption of 0.38 mJ. Moving to the maximum performance configuration (Figure 3-B), the inference time gets reduced to 6.3 ms under the same average power, leading to 0.63 mJ per frame. Overall, these results show an improvement of 8.5 $\times$  on the network’s

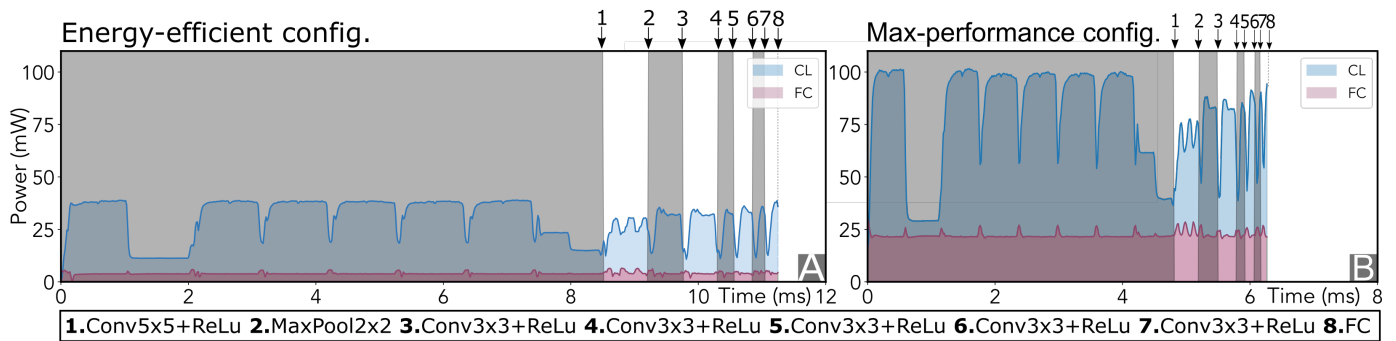


Figure 3. GAP8 power waveforms executing the smallest Tiny-PULP-Dronet ( $\gamma = 0.125$ ). (A) most energy-efficient SoC’s configuration – FC@50 MHz, CL@100 MHz, VDD@1.0 V – and (B) the maximum performance one – FC@250 MHz, CL@175 MHz, VDD@1.2 V.

inference time when compared to the baseline PULP-Dronet, which takes 96 ms and 52 ms to run an inference under the energy-efficient and maximum performance SoC configurations, respectively. Ultimately, we improve the frame-rate of PULP-Dronet from 10 frame/s to 89 frame/s on the energy efficient configuration, and from 19 frame/s to 160 frame/s, on the maximum performance one.

Lastly, we analyze the execution of the first  $5 \times 5$  convolution, which takes about 75% of the total network’s execution time on the smallest Tiny-PULP-Dronet ( $\gamma = 0.125$ ). This layer processes a  $200 \times 200 \times 1$  input image and outputs a  $100 \times 100 \times 4$  feature map, resulting in 1MMAC operations, which corresponds to the 70% of the total network’s operations, partially explaining its higher execution time over the others. However, alongside the reduction by  $27\times$  of the network’s MAC operations w.r.t. the baseline, we only witness a latency reduction of  $8.5\times$ . This non-linear scaling is due to inevitable non-idealities: *i*) the Height-Width-Channel data layout limits the input feature map data reuse, being proportional to the layer’s output channels number, i.e., only 4, *ii*) the marshaling stage required by the convolution for padding and constructing the input’s flattened buffer adds up to 45% of the total layer execution. Ultimately, with a peak  $8.5\times$  throughput improvement, Tiny-PULP-Dronets enable a faster reactivity of the nano-UAV when autonomously navigating the environment.

#### IV. CONCLUSION

The limited payload and computational power of nano-UAVs prevent high-level onboard intelligence, such as multi-tasking execution, which is still out of reach.

This work presents a general methodology that leverages the CNN’s sparsity and overfitting to squeeze both memory footprint and computational effort. By applying our methodology to the SoA PULP-Dronet CNN for autonomous driving, we introduce its Tiny-PULP-Dronet variants. These CNNs show a reduced memory burden ( $50\times$  smaller) and computational complexity ( $27\times$  lower) vs. the original model while *i*) preserving the same regression performance, *ii*) having minimal accuracy degradation (6% at most), and ultimately leaving sufficient resources for faster and lighter inference on multi-tasking autonomous nano-drones.

#### ACKNOWLEDGMENTS

We thank A. Giusti and A. Burrello for their support.

#### REFERENCES

- [1] M. J. Anderson, J. G. Sullivan, J. L. Talley, K. M. Brink, S. B. Fuller, and T. L. Daniel, “The “smellicopter,” a bio-hybrid odor localizing nano air vehicle,” in *2019 IEEE/RSJ International Conference on Intelligent Robots and Systems (IROS)*, 2019, pp. 6077–6082.
- [2] D. Palossi, N. Zimmerman, A. Burrello, F. Conti, H. Müller, L. M. Gambardella, L. Benini, A. Giusti, and J. Guzzi, “Fully onboard ai-powered human-drone pose estimation on ultra-low power autonomous flying nano-uavs,” *IEEE Internet of Things Journal*, pp. 1–1, 2021.
- [3] H. Müller, D. Palossi, S. Mach, F. Conti, and L. Benini, “Fünfiiberdrone: A modular open-platform 18-grams autonomous nano-drone,” in *2021 Design, Automation Test in Europe Conference Exhibition (DATE)*, 2021, pp. 1610–1615.
- [4] L. Bigazzi, M. Basso, S. Gherardini, and G. Innocenti, “Mitigating latency problems in vision-based autonomous uavs,” in *2021 29th Mediterranean Conference on Control and Automation (MED)*, 2021, pp. 1203–1208.
- [5] R. Bonatti, C. Ho, W. Wang, S. Choudhury, and S. Scherer, “Towards a robust aerial cinematography platform: Localizing and tracking moving targets in unstructured environments,” in *2019 IEEE/RSJ International Conference on Intelligent Robots and Systems (IROS)*, 2019, pp. 229–236.
- [6] P. Foehn, D. Brescianini, E. Kaufmann, T. Cieslewski, M. Gehrig, M. Muglikar, and D. Scaramuzza, “Alphapilot: autonomous drone racing,” *Autonomous Robots*, vol. 46, no. 1, pp. 307–320, 2022.
- [7] M. Giurfa and R. Menzel, “Insect visual perception: complex abilities of simple nervous systems,” *Current Opinion in Neurobiology*, vol. 7, no. 4, pp. 505–513, 1997.
- [8] J. E. Kooi and R. Babuška, “Inclined quadrotor landing using deep reinforcement learning,” in *2021 IEEE/RSJ International Conference on Intelligent Robots and Systems (IROS)*, 2021, pp. 2361–2368.
- [9] G. Shi, W. Hönig, X. Shi, Y. Yue, and S.-J. Chung, “Neural-swarm2: Planning and control of heterogeneous multirotor swarms using learned interactions,” *IEEE Transactions on Robotics*, pp. 1–17, 2021.
- [10] V. Niculescu, L. Lamberti, D. Palossi, and L. Benini, “Automated tuning of end-to-end neural flight controllers for autonomous nano-drones,” in *2021 IEEE 3rd International Conference on Artificial Intelligence Circuits and Systems (AICAS)*, 2021, pp. 1–4.
- [11] K. He, X. Zhang, S. Ren, and J. Sun, “Deep residual learning for image recognition,” in *2016 IEEE Conference on Computer Vision and Pattern Recognition (CVPR)*, 2016, pp. 770–778.
- [12] T. Hoefler, D. Alistarh, T. Ben-Nun, N. Dryden, and A. Peste, “Sparsity in Deep Learning: Pruning and growth for efficient inference and training in neural networks,” *Journal of Machine Learning Research*, vol. 22, no. 241, pp. 1–124, Sep. 2021.
- [13] L. Sigrist, A. Gomez, R. Lim, S. Lippuner, M. Leubin, and L. Thiele, “Rocketlogger: Mobile power logger for prototyping iot devices: Demo abstract,” in *Proceedings of the 14th ACM Conference on Embedded Network Sensor Systems CD-ROM*, ser. SenSys ’16. New York, NY, USA: Association for Computing Machinery, 2016, p. 288–289.